



Naesgaard, E., Amini, A., Uthayakumar, U.M., and Fellenius, B.H., 2012. "Long piles in thick lacustrine and deltaic deposits. Two Bridge Foundation Case Histories." Full-scale Testing in Foundation Design, M.H. Hussein, R.D. Holtz, K.R. Massarsch, and G.E. Likins, eds., Geotechnical Special Publication 227, 404-421. ASCE Geoinstitute Geo-Congress, Oakland March 25-29, 2012, State of the Art and Practice in Geotechnical Engineering, ASCE, Reston, VA.

Long Piles in Thick Lacustrine and Deltaic Deposits. Two Bridge Foundation Case Histories

Ernest Naesgaard¹⁾, PhD., P.Eng., P.E., M.ASCE
 Ali Amini²⁾, PhD., P.Eng.,
 Uthaya M. Uthayakumar³⁾, PhD., P.Eng.
 Bengt H. Fellenius⁴⁾, Dr.Tech., P.Eng., M.ASCE

¹⁾Naesgaard Geotechnical Ltd., RR1 Site I-38, Bowen Island, BC, V0N 1G0
 <ernestn@shaw.ca>

²⁾Naesgaard Geotechnical Ltd., 2547 Shelley Rd., North Vancouver, BC, V7H 1K1
 <ali.amini@shaw.ca>

³⁾EXP Services Inc., 7025 Greenwood St., Burnaby, BC, V5A 1X7
 <Uthaya.Uthayakumar@exp.com>

⁴⁾Consulting Engineer, 2475 Rothesay Avenue, Sidney, BC, V8L 2B9
 <Bengt@Fellenius.net>

ABSTRACT. Two recent bridge projects in British Columbia highlight the importance of having well-instrumented pile loading tests as part of piled foundation design. First case is the 1.5 km long, five-lane W.R. Bennett Bridge in the challenging Okanagan Lake soil profile with soft and loose to medium dense silts and silty sands to depths over 100 m. Five 610-mm diameter open- and closed-toe test piles were driven to 45 m depth. Pile dynamics tests were performed for all five test piles and a static loading test was carried out on the center pile, driven closed-toe. The importance of considering residual load in the test interpretation is illustrated.

Second case is the 2.6 km long (main bridge and approaches) six-lane, cable-stayed Golden Ears Bridge over the Fraser River delta. Soils consisted of thick, potentially liquefiable sands, overlying near-normally consolidated soft to stiff clayey silts and silty clays to over 120 m depth. The south approach and main span piers are founded on 2.5 m diameter bored piles of up to 85 m length. Four loading tests were carried out for this project. One of the tests, a 74 m deep 2.5 m diameter pile loaded with bi-directional O-cells is described and the test results, their interpretation, and general foundation design methods and considerations are presented.

1. INTRODUCTION

Two major bridges in British Columbia, Canada, the W.R. Bennett Bridge owned by BC Ministry of Transportation (MoT) and the Golden Ears Bridge owned by Metro Vancouver's regional transportation authority (TransLink) were recently constructed and were opened to the public in May 2008 and June 2009, respectively. No suitable toe bearing stratum was found, to the maximum depth investigated, at either site and both bridges were founded on relatively long piles with substantial shaft resistance components.

W.R. Bennett Bridge is founded on 30 to 50 m long, 610 mm and 914 mm diameter open-toe steel pipe piles driven into thick normally consolidated lacustrine silt and silty sand soils. The Golden Ears Bridge main crossing and south approach are founded on 75 to 85 m long, 2.5 m diameter concrete bored piles in sand overlying normally to lightly over-consolidated clayey silts and silty clays deposited in marine environment.

Loading tests on well instrumented piles were carried out at both sites given the weak ground conditions, importance of the structures, high load demands, large variability in capacities from alternative calculation procedures, and, at the Golden Ears Bridge site, lack of local experience with the pile construction methodology. At the Bennett Bridge, the loading tests were by MoT and at Golden Ears Bridge they were by the design-build contractor.

2. W.R. BENNETT BRIDGE PILE LOADING TEST

2.1 General

A previous 1.5 km long three-lane Okanagan Lake Bridge was replaced with a new five lane structure (Figure 1), named W.R. Bennett Bridge. The new bridge has floating and pile supported fixed structure parts, a water crossing of 920 m, water depths up to 45 m, and weak compressible foundation soils. The structures on the west side, including the west abutment are supported on 30 m to 50 m long, 914 mm diameter, open-toe pipe piles. The east abutment is supported on 45 m long, 610 mm diameter, open-toe pipe piles. A pile test programme involving 610 mm diameter pipe piles was conducted in April 1999 to assess axial pile capacity and pile drivability (Naesgaard et al. 2006).

The test programme for the foundations of the W.R. Bennett Bridge involved driving of five 610 mm diameter, 12.7 mm wall, steel pipe piles to 45 m below the lake bottom. An axial static loading test was carried out on the central pile which was instrumented with strain gages and telltales. Pile driving analyzer (PDA) testing was carried out on all five piles. Following the axial tests, a lateral test was carried out on two of the piles. The test results provided data and insight on: the effect of vibratory driving on capacity, residual loads and load distribution within the pile, comparison of capacity of open-toe and closed-toe piles, comparison of axial capacity from dynamic and static test, and comparisons of measured axial capacity to those calculated using

different design methods. Developed residual load and general pile behaviour could be simulated by a relatively simple, elastic-plastic, dynamic numerical model.

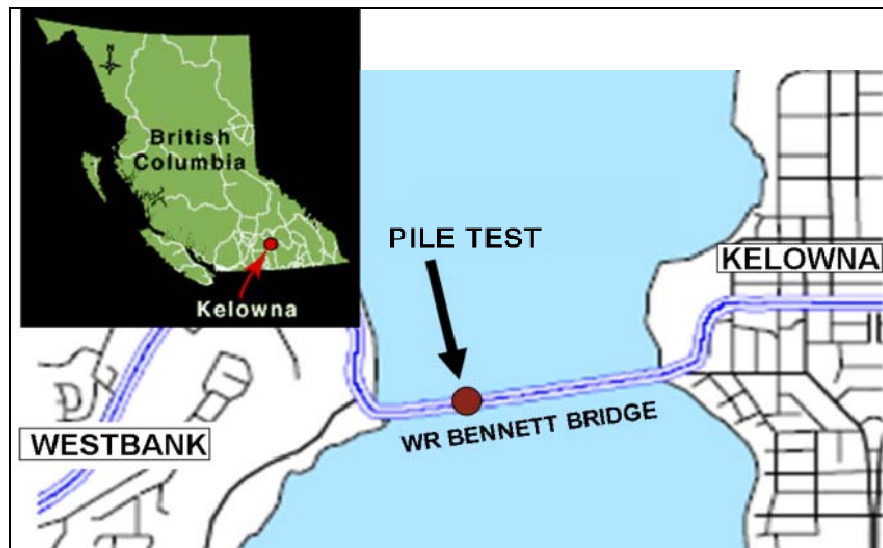


Fig. 1 Location of WR Bennett Bridge and pile test

The soils at the site are lacustrine and glacio-lacustrine sediments draped over the underlying Pleistocene fjord-like topography (Nasmith 1962; Fulton 1975; and Eyles et al. 1990). At the pile test location, near normally consolidated sediments are over 60 m thick with an 8 m surficial soft silt layer above 17 m of sandy silt overlying sand. Figure 2 illustrates that the silt and sand are interlayered with thin bands or zones of coarser and finer material. The relatively young, normally consolidated silt layers have water contents in the range of 23 % through 74 %, liquid limits 23 % through 65 %, and plastic limits 17 % through 44 %. Lake water depth at pile test was 6.5 m and the pore pressure distribution is hydrostatic to the lake level.

2.2 Test Pile Installation

Piles were installed from a barge using an 80-tonne crawler crane. Layout of the test piles in plan and profile is shown in Figure 3. The five pipe piles (P1 to P5 in Figure 3) were supplied in 18.3m lengths and spliced on site. The end plates on the closed-toe piles were welded flush with the OD of the pipe. Three pile hammers were used: a 3,855 kg drop hammer, a 5,445 kg drop hammer, and an APE 44-50 vibratory hammer. All five piles were re-struck eight days after the axial loading test (on Pile 1) with a Delmag D62 diesel hammer and/or large drop hammer. Details of the pile installation are summarized on Table 1 and Figure 4.

2.4 Pile Driving Analyzer Testing

Pile driving analyzer (PDA) testing was conducted at end of initial driving, EOID, and at re-strike 23 days after EOID (8 days after the static loading test). Small and large drop hammers were used for EOID testing and large drop hammer and Delmag

D62 diesel hammer were used for the re-strike testing. CAPWAP analyses were conducted to determine pile capacities from the PDA records (see Table 2). Residual or locked-in loads were not considered in PDA/CAPWAP shaft and toe capacities in Table 2.

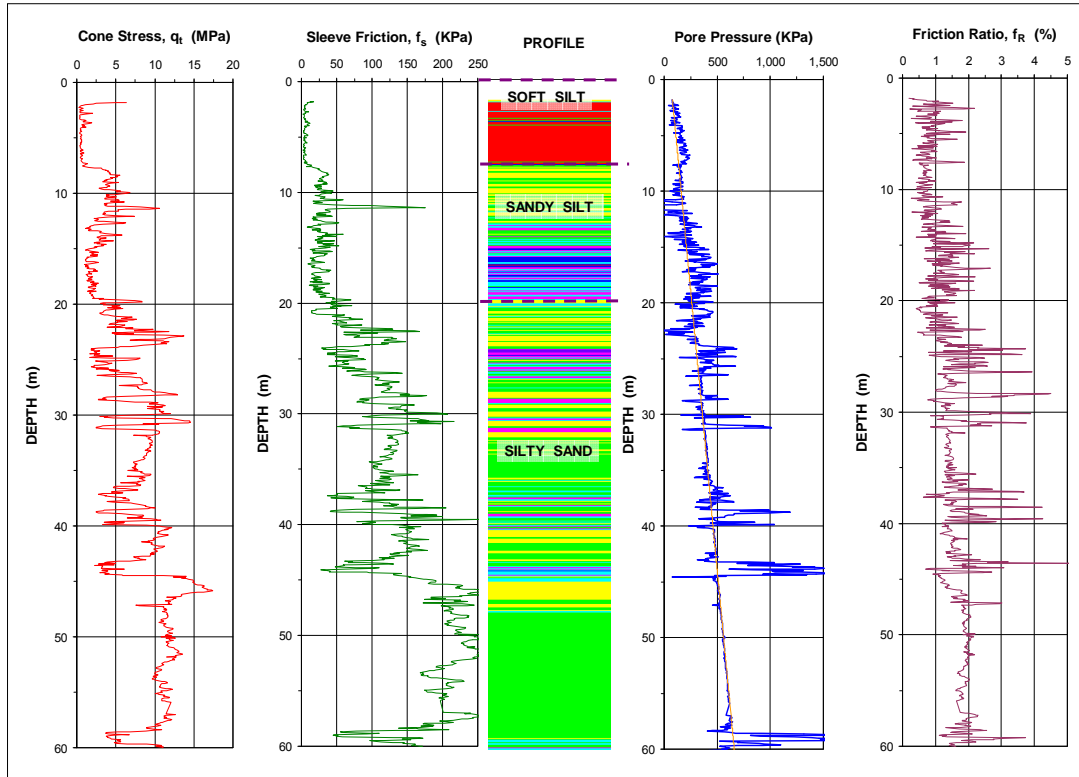


Fig. 2 CPTU diagram and soil profile

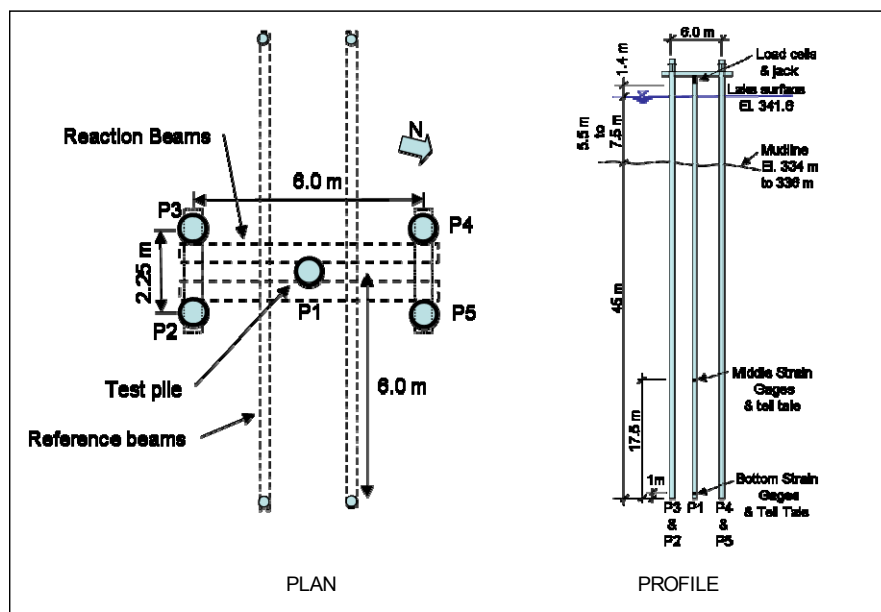


Fig. 3 Layout of piles in plan and profile

Table 1 Summary of pile installation and testing sequence

Time relative to EOID (days)	P1	P2	P3	P4	P5
	CLOSED-IOE	OPEN-IOE	CLOSED-IOE	CLOSED-IOE	OPEN-IOE
-8	-	D _s (0-8.2)	-	D _s (0 - 9.1)	-
-7	D _s (0 - 9.1) S(18.9)	S(18.0)	D _s (0-9.1) S(18.9)	S(18.9)	D _s (0-90.1)
-6	V(9.1-21.0) (20min)	V(8.2-27.4) (1.2min)	-	V(9.1-22.3) (30min)	-
-5	D _s (21.0-28.4)	-	D _s (9.1-27.4)	D _s (22.3-27.4)	-
-2	-	S(37.2)	S(37.2)	S(37.2)	S(37.8)
-1	S(38.2)	D _s (27.4-37.5)	D _s (27.4-37.8)	D _s (27.4-43.0)	D _s (28.0-43.6)
EOID	D _s (28.4-44.5) PDA w/ D _s & D _i	D _s (37.5-44.5) PDA w/ D _i	D _s (37.8-43.4) PDA w/ D _i	D _L (43.0-43.1) PDA w/ D _i	D _L (43.6-43.7) PDA w/ D _i
5	-	-	CONCRETE FILL	CONCRETE FILL	-
15	AXIAL LOADING TEST	-	-	-	-
20/21	-	-	LATERAL TEST	LATERAL TEST	-
23 re-strike	PDA w/ D ₆₂	PDA w/ D ₆₂	PDA w/ D _L	PDA w/ D _L	PDA w/ D ₆₂
Toe elev.(m)	291.0	291.0	292.0	292.4	291.8

Notes

D_s = 3,855-kg hammer with 2.5 m drop;
D_L = 5,445-kg hammer with 2.5 m drop;
V = APE 44-50 Vibratory hammer
S(18.9) = Splice at 18.9 m from toe of pile
D₆₂ = Delmag D62 diesel hammer

(21.0-28.4) = driven from 21.0 m through 28.4 m depth with indicated hammer
(20 min.) = Duration of vibratory driving
EOID = End Of Initial Driving;
PDA = Pile Driver Analyzer testing

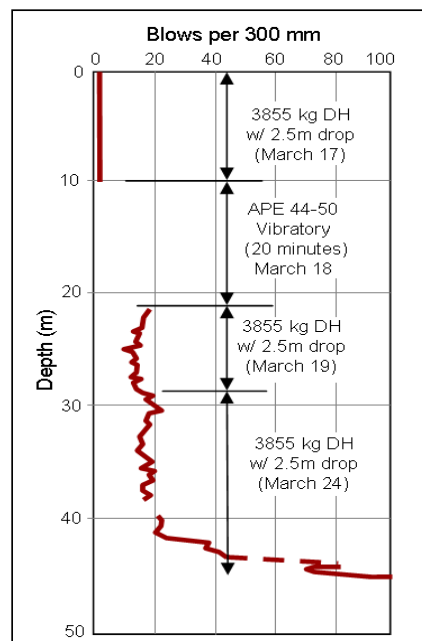
**Fig. 4 Driving record of Pile P1**

Table 2 Summary of axial capacities (MN) of piles at W.R. Bennett Bridge

Case	Pile No.	PDA testing		Calculated Capacity						Static Loading Test ⁽¹⁾ (Day 15)	
		EOID (day 0)	Restrike (day 23)	LCPC	E-F	D	M	S	API	post-driving residual stresses	
										ignored	included
Pile shaft capacity (MN)	P1	2.8	3.1 to 2.9	2.6	4.3	7.5	2.2	3.2	4.0	2.2 to 2.3	1.4 to 1.5
	P2	3.3 to 3.7	3.0								
	P3	1.8	3.0								
	P4	2.6 to 2.8	3.0 to 3.5								
	P5	2.6 to 2.9	3.2								
Pile toe capacity (MN)	P1	1.2	1.1 to 1.4	1.7	2.5	1.5	2.3	1.9	1.4	1.4 to 1.7	2.2 to 2.5
	P2	0.4 to 0.5	1.1								
	P3	1.2	0.9								
	P4	0.4	0.8 to 0.9								
	P5	0.3 to 0.4	0.9								
Total capacity (shaft and toe) (MN)	P1	4.0	4.2 to 4.3	4.3	6.8	9.1	4.5	5.1	5.4	3.6 to 4.0	3.6 to 4.0
	P2	3.8 to 4.0	4.1								
	P3	3.0	4.0								
	P4	3.0 to 3.2	3.8 to 4.4								
	P5	3.0 to 3.2	4.2								

LCPC = LCPC CPT-method; E-F = Eslami-Fellenius CPTU method; D = Dutch CPT-method; M = Meyerhof CPT-method; D = European (Dutch) CPT-method; s = Schmertmann CPT-method; API = API RP2A (1993) CPT-method.

Notes: (1) Shaft and toe load distribution has been corrected by subtracting 110 kN to compensate for lower strain gages being one metre above the pile toe. Piles P1, P3, and P4 were closed-toe and P2 and P5 were open-toe. (2) Calculated capacities vary according to parameters chosen. Listing of the different values of calculated capacities do not imply that one method is better than another, but are rather intended to show the variability in commonly used design methods.

2.4 Axial Pile Loading Test

2.4.1 Instrumentation

Pile P1 was selected for a static loading test. This pile was instrumented with vibrating wire strain gages (four per level) and telltales prior to driving of the pile. During the test, pile axial movement was monitored using six displacement transducers (LVDTs) that were attached to an independent steel reference frame supported by four 324 mm diameter pipe piles (Figure 3). Pile vertical movement was also measured by sighting with a transit onto scales attached to the test and reaction piles. The transit was set on shore 18 m from the test piles. This redundancy of data proved to be useful as the LVDTs reached the end of their travel several times during the test and had to be reset. Axial load was measured using two calibrated 2.7 MN load cells in parallel on the pile head. Jack pressure was also monitored.

2.4.2 Test Procedure

The test was conducted on Pile P1 in three stages (Figures 5, 6, and 7). The first stage consisted of loading the pile head in increments of 225 kN with 15 minute load-holding (duration) until an ultimate resistance of 3,700 kN. The second stage consisted of cycles of loading and unloading between 2,000 kN and 3,000 kN. The rate of loading (as governed by the jack rate) was about five minutes per cycle; unloading was fast. The third stage started from the lower load of the 21st cycle,

consisting of an incremental quick loading to an ultimate resistance followed by complete unloading in quick steps. The maximum load attained load in the third stage was 4,000 kN, but it could not be sustained. Table 2 presents a summary of axial capacities from static test, PDA, and calculations. The pile capacity according to the Davisson offset limit (CFEM 2006) was 3,600 kN.

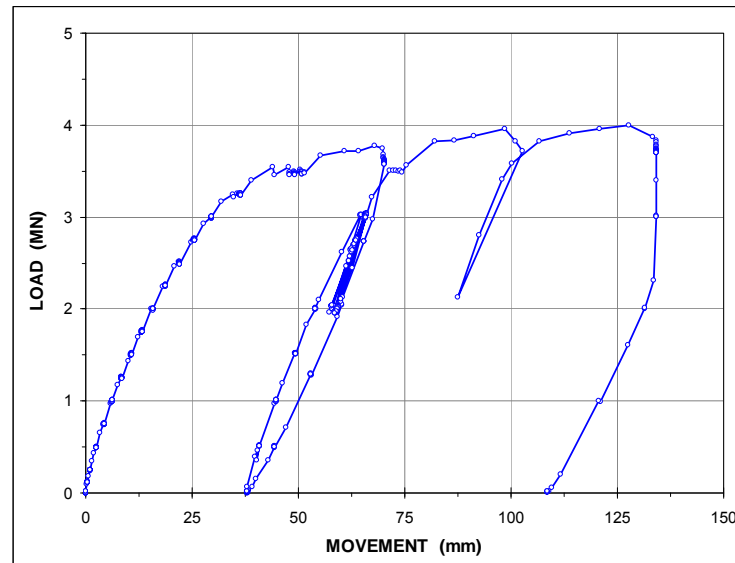


Fig. 5 Pile head load-movement in the static loading test on Pile P1

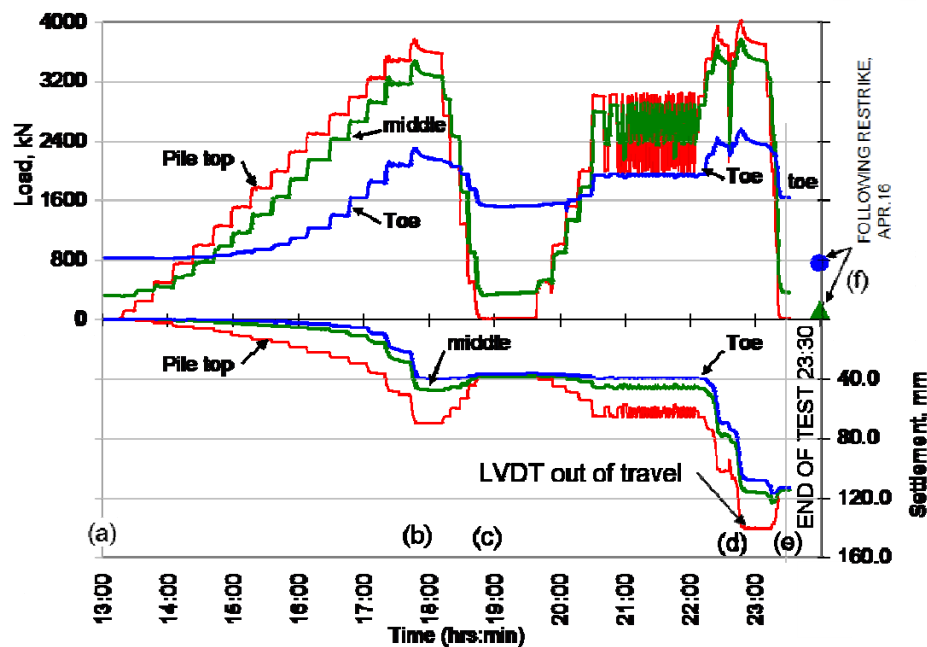


Fig. 6 Load and movement versus time for axial load test on pile P1 (April 16). Toe readings are from gages 1 m above the pile toe and middle readings are from gages located 17.5 m above the toe.

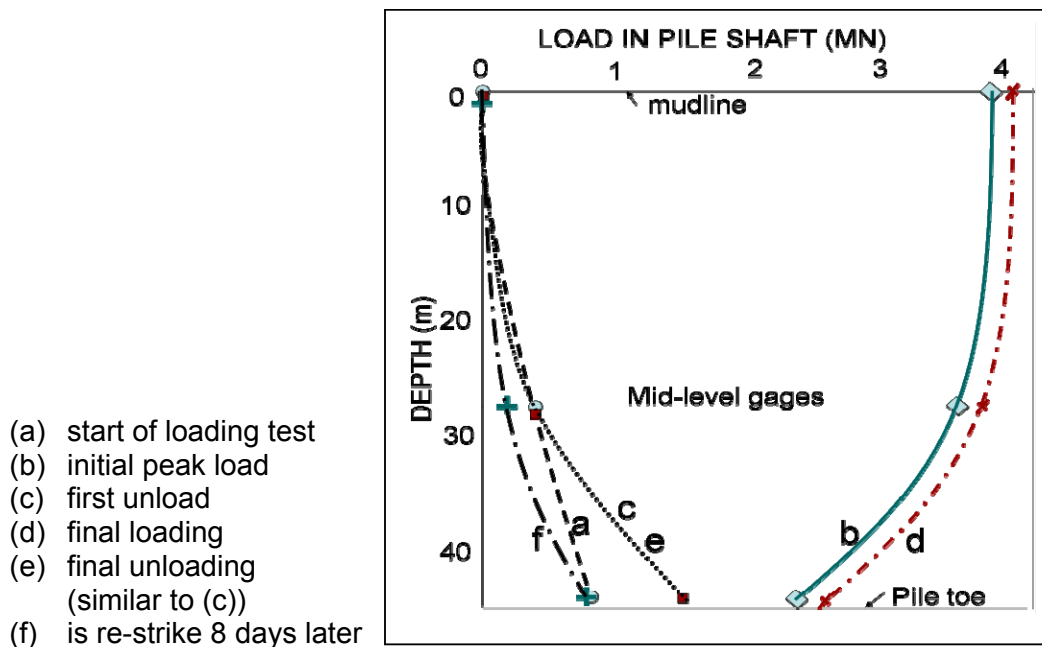


Fig. 7 Pile 1 - Induced load distribution inferred from load at pile head and strain gage values ('a' to 'f' in Fig. 7 correspond to (a) to (f) in Fig. 6).

2.4.3 Calculated Axial Capacity

Pile capacities were calculated from the CPTU sounding data using five alternative methods: Eslami-Fellenius (Eslami and Fellenius 1997), European (Dutch) (De Ruyter and Beringen 1979), Meyerhof (Meyerhof 1976), Schmertmann (Schmertmann 1978), API methods (API, RP 2A-WSD 1993), and a modified LCPC method (Bustamante and Gianceselli 1982). The Eslami and Fellenius method applies cone stress corrected for pore pressure, q_t , whereas Meyerhof, European, and Schmertmann methods apply the uncorrected cone stress, q_c . The original LCPC method was modified to use q_t instead of q_c and to use soil type from software UBCINT (v.5.2).

2.4.4 Discussion

Residual or locked-in load: The importance of residual loads in assessing the correct load distribution in piles was noted as early as 1963 by Nordlund (1963); and Hunter and Davisson (1968); overviewed by Mouta da Costa et al. (2001); and discussed by Fellenius et al. (1978); and Fellenius (2002a, 2002b). Residual loads can be induced in the pile by driving or jacking and by post-driving consolidation settlement of the soil. Driving impact causes a compression wave down the pile. Following wave passage, the pile attempts to rebound to its former stress state; however the soil around the pile prevents full rebound and induces residual loads in the pile. In a similar manner, the soil around the shaft prevents full rebound of the pile shaft and locks in stresses on unloading the pile after static loading. Additional load can also be locked in due to re-consolidation of the soil after the driving and, if strain softening or creep occurs, there may be release of residual load with time (Fellenius et al. 2004).

Pile installation at this site induced a residual load of 835 kN near the pile toe and 400 kN at 17.5 m above the toe (Figures 6 and 7) to give the load distribution 'a' in Figure 7. Applying load to the pile head compresses the pile shaft and initially reduces negative direction shear forces along the pile. At approximately Time 14:30h (Figure 6), there is almost no shear force along the pile and nearly all the applied load is resisted by the pile toe. Continued loading after Time 14:30h causes positive shaft resistance to build up along the pile shaft until the pile is near its capacity, Curve 'b' in Figure 7. At Curves 'c' and 'e', the load on the pile head is zero and the residual load near the pile toe is almost double what it was at the start of the test. This is indicative of residual load from static pushing being higher than that from impact driving. When the pile was re-struck 8 days after the loading test (Curve 'f' in Figure 7), the residual load reduced to values similar to those at end of initial driving and at start of the loading test. When residual load is considered, approximately 60% of Pile P1 total resistance is taken by the toe and only 40% by the shaft. If the strain gages had been zeroed at the start of the test and residual load not considered, then, incorrectly, 40% of the load would be attributed to the toe and 60% to the shaft. The proper choice will reflect in design parameters back-calculated from the loading test. With residual load, an effective stress β -coefficient (CFEM 2006, Fellenius 2009) of 0.10 and toe bearing coefficient, N_t , of 22 are back-calculated. If initial residual load is ignored, the values would be 0.15 and 9. Clearly, extrapolation to other lengths and diameters may lead to incorrect results if the residual loads are not considered.

The increase in capacity between (b) and (d) in Figure 7 is nearly all due to increase of the toe value as the pile toe moved deeper into the relatively strong sandy layer at approximately 45 m depth (Figure 2).

Comparison of Pile Capacities: Correct pile capacity is the capacity determined in a static loading test. As shown in Table 2, agreement is good (within $\pm 15\%$) between the PDA "CAPWAP" capacity (at re-strike) and that from the pile loading test (3.9 MN). Capacities calculated from the CPT sounding, using modified LCPC and Meyerhof methods also correlate well with the static loading test results. However, when studying the distribution, agreement is not as good. The scatter in the calculated shaft capacities was large and all methods over-estimated shaft capacity. As to toe resistance, the cone methods were within $\pm 40\%$ of the toe resistance with the Eslami and Fellenius method and Meyerhof method being close to the static test value. Back-calculated effective stress parameters, β of 0.10 and N_t of 22, are lower than commonly quoted values (CFEM 2006).

2.6 Numerical Emulation of Pile Installation and Axial Loading Test

A numerical simulation of the installation (driving) and axial loading of the test pile was carried out using the program FLAC (Itasca 2005). The two-dimensional plane strain model shown in Figure 8 has a 1 m by 1 m mesh, a Mohr Coulomb soil constitutive model, and pile structural elements. A shear interface on the sides of the pile is modelled with a t-z like elastic-plastic springs between the pile structural nodes

and adjacent soil nodes. The strength of the interface is proportional to the normal stress on the pile. Driving of the pile was emulated by actual modelling of the hammer with elastic elements and placing interfaces between the hammer and the pile. Pile driving is carried out in FLAC's dynamic mode by lifting the hammer and dropping it, much as is done in the real world. The pile loading test was simulated by applying a small downward velocity to the pile head and monitoring axial load in the pile. With this model, and as shown in Figure 9, the pile was given two blows (to simulate the blows at end-of-driving). The pile was then statically load tested and, after the loading test, the pile was given two additional blows to simulate re-striking. Much of the behavior observed in the actual pile installation could also be seen in the numerical model, including the build-up of residual load in the pile due to driving, increase in residual load and eventual pile-plunging due to static loading, and reduction of residual load due to re-striking following static testing. The cycling of load at the pile head showed no change of load at the pile toe when the cyclic loads were smaller than the pile shaft resistance. The load verses time plot from the numerical model (Figure 9) has similar characteristics to that measured on the actual test pile (Figure 6).

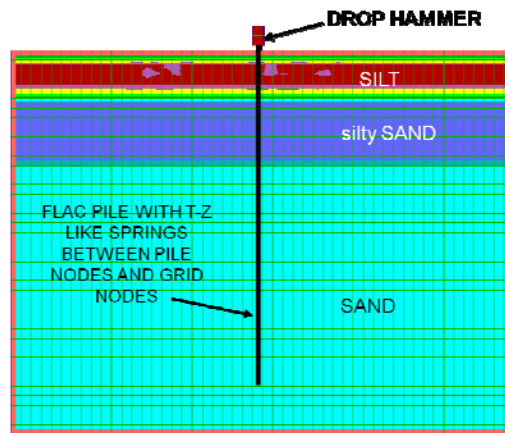


Fig. 8 Two-dimensional FLAC model of pile installation and loading test

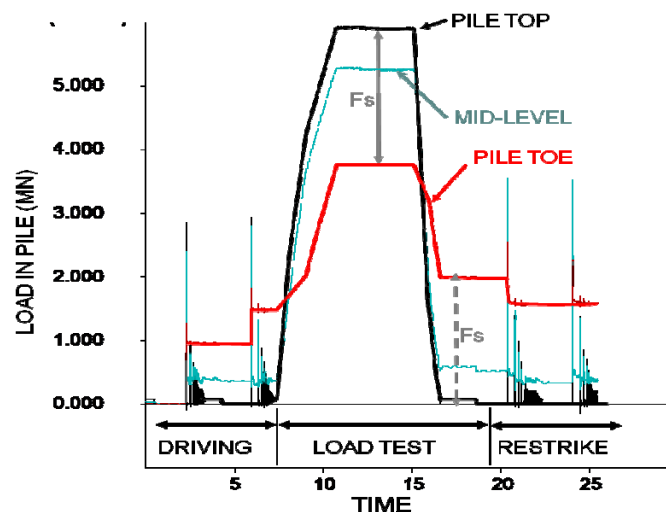


Fig. 9 Pile load verses time as calculated by the numerical model.

3.0 GOLDEN EARS BRIDGE PILE LOADING TESTS

3.1 General

The Golden Ears Bridge is a new cable-stayed bridge over the Fraser River connecting Maple Ridge and Pitt Meadows to Langley and Surrey in BC, Canada, completed in 2009 (Amini et al. 2008) by Golden Crossing Constructors Joint Venture. The bridge is 2.6 km in length and includes a 970 m river crossing (Figure 10).

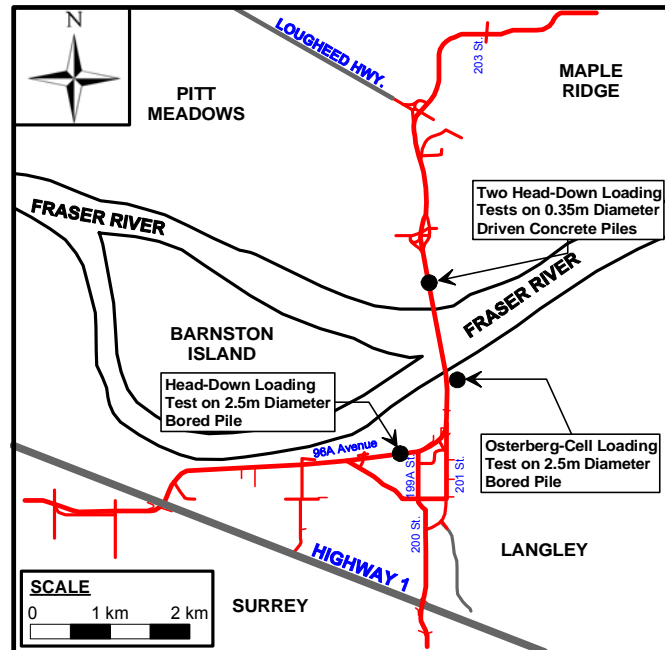


Fig. 10 Location of Golden Ears Bridge and pile test

The main bridge has four marine piers each supported on groups of 12 bored piles of 2.5 m diameter constructed to 75 to 85 m depth. The south approach structure and ramps are also on 80 m long, 2.5 m diameter bored piles. The design required an unfactored ultimate axial resistance of up to about 60 MN for each pile.

The north approach structures are supported on groups of 350 mm square, ordinary reinforced, precast concrete piles driven to 12 to 36 m depth. All piles are shaft-bearing in post-glacial normally consolidated (NC) to lightly over-consolidated (OC), soft to stiff silty clay with a surface layer of loose to dense sand in places. Different methods of pile capacity calculation resulted in a wide range of potential axial capacities. To calibrate the calculation methods and confirm capacity, four static loading tests were completed. This included one head-down test and one O-Cell test (Osterberg 1989; 1998) on 2.5 m diameter, strain-gage instrumented bored piles, one constructed to 74.5 m depth and the other to 32.0 m depth. Head-down static loading test was also performed on two 350 mm diameter driven precast concrete piles (not instrumented).

This paper reports the results of the O-cell loading test on the 2.5m diameter 74.5 m long bored pile but also mentions results from some of the other tests in discussion. More data and detail discussion on all the tests can be found in Amini et al. (2008).

The soils at the location of the O-cell tested pile consisted of 17 m of loose to medium silty sand to sand overlying 21 m of medium to dense fine to medium sand overlying stiff NC to lightly OC silty clay with intermittent thin silty sandy layers to depth beyond 100 m. The groundwater table was at 2.1 m depth below ground surface. The pore water pressure in the upper sand units was hydrostatic while there were artesian pressures in the underlying clay (70 kPa in excess of hydrostatic pressure at 100 m depth). Figure 11 shows profiles of Atterberg limits and water content, cone (CPT) bearing stress, and CPT derived undrained shear strength.

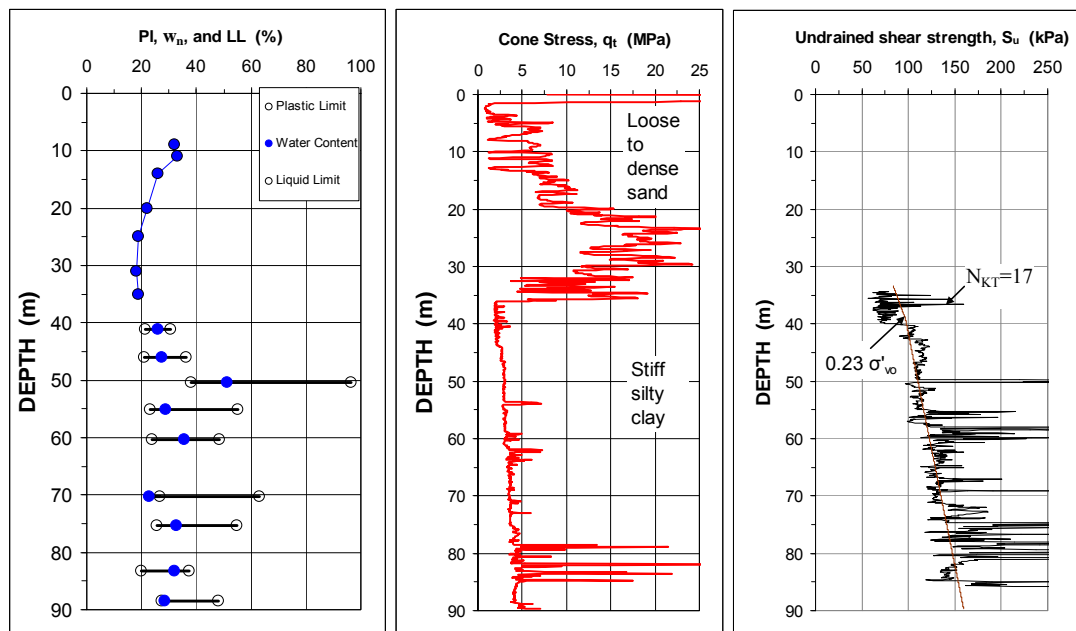


Fig. 11 Soil consistency limits, cone stress, and undrained shear strength profile for O-cell pile loading test on a 2.5m diameter, 74.5m long bored pile.

3.2 Osterberg-Cell Loading Test on a 2.5 m Diameter 74 m Long Bored Pile

The test pile was constructed by vibrating a permanent 2.5 m diameter steel casing to a depth of 21 m and then excavating with a spherical grab. Polymer slurry with a positive head of about 7.5 m above the water table was used to help maintain stability of the hole. From sonar caliper tests, an average shaft diameter of 2.6 m and a general inclination of about 1 % were found. Two O-cell assemblies and corresponding instrumentation were attached to the reinforcing steel cage by Loadtest Inc., Florida. The lower O-cell assembly at 70.5 m depth had a capacity of 18.7 MN and the upper O-cell assembly at 44 m depth had a capacity of 48 MN. The instrumentation included vibrating wire displacement transducers positioned between the O-cell assemblies and vibrating-wire strain gage pairs at nine levels in the pile. The shaft was concreted through a tremie pipe extending to the bottom of the pile.

The O-cell loading test was performed 30 days after the pile was completed with load increments added every ten minutes. Initially (Stage 1), the lower O-cell was expanded with the upper O-cell locked. Then, in Stage 2, the upper O-cell was expanded with the lower cell open and vented. Finally, in Stage 3, the upper O-cell was expanded with the lower O-cell closed.

The observed upward and downward load-movements from Stages 1 and 2 are shown in Figure 12. In Stage 1, when the O-cell load was 7.1 MN, the pile section below the lower O-cell started to tilt. Attempts to adjust the tilt were not successful, and the cells were unloaded from a maximum load of 8.0 MN at 140 mm downward movement. The downward load-movement curve suggests that, prior to the start of the test, about 3.5 MN residual load existed in the pile at the level of the lower O-cell. This could have been locked-in during the concreting process, or alternatively the 3.5 MN could be the shaft resistance between the bottom O-cell and pile toe.

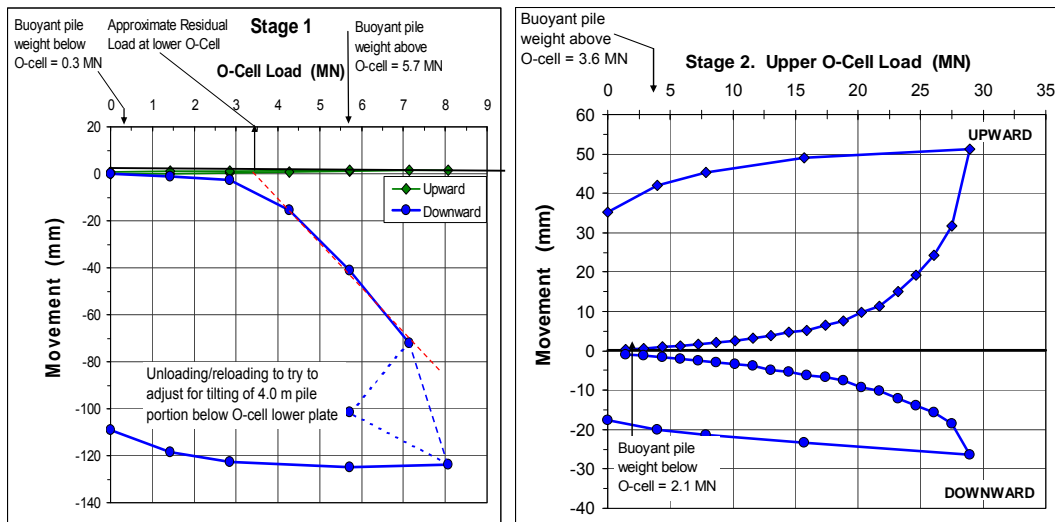


Fig. 12 Stage 1, lower O-cell load-movements and Stage 2, upper O-cell load-movements for the Golden Ears O-cell test pile.

The Stage 2 (lower O-cell open and vented) upward and downward load-movement curves from the upper O-cell level are also shown in Figure 12. The pile was loaded in 20 increments to a maximum O-cell load of 29.0 MN.

Both the upper and the middle segments are considered to have reached the ultimate shaft resistance. Therefore, the planned next test stage, Stage 3, was cancelled. The upper segment is considered to have reached the ultimate resistance at the 29.0 MN maximum load minus the 3.6 MN buoyant weight to give a shaft resistance of 25.4 MN. The upward movement was 50 mm. The 28.2 MN shaft resistance of the middle segment was interpreted to be the O-cell load measured before the lower cells engaged (26 MN) plus buoyant weight of middle segment (2.1 MN). The downward movement of the middle segment was then 25 mm. The pile shaft resistance at depths 44 m, 70.5 m and 74.5 m were thus interpreted as 25.4 MN, 53.6 MN, and 58.1 MN, respectively.

The shaft resistance values were used to calibrate various pile capacity calculation methods, including the total stress Alpha method (pile shaft resistance = alpha (α) times undrained strength (S_u)), effective stress Beta method (pile shaft resistance = beta (β) times vertical effective stress (σ'_{vo})) and CPT and CPTU methods. Figure 13 shows the O-cell loads, loads interpreted from the strain-gage values, and shaft resistance distributions calculated from the case-adjusted CPT based methods (LCPC and E-F) and the API Alpha method (API 2000). Saturated unit weights of 20 kN/m^3 and 17.5 kN/m^3 were used for the sand and clay, respectively.

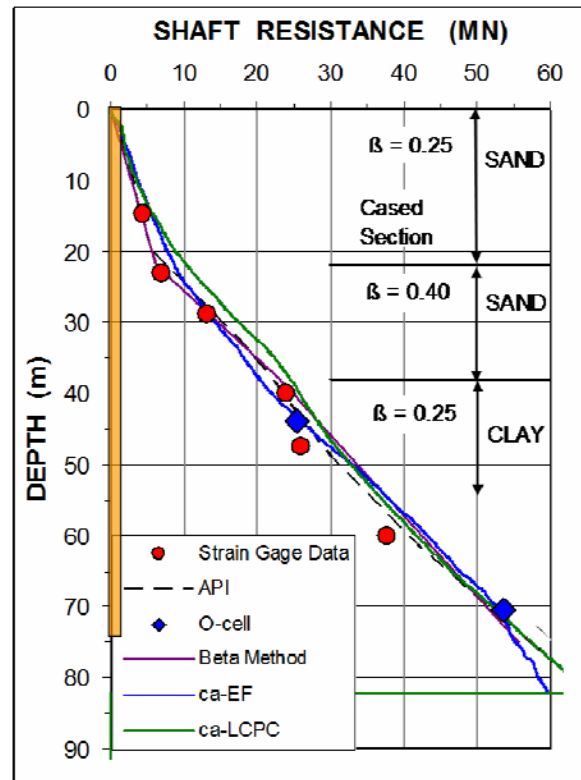


Fig. 13 Shaft resistance in O-cell test pile showing strain gage and O-cell data compared to best-fit capacity calculation methods

An alpha value near unity was back calculated for the normally consolidated clay ($S_u/\sigma'_{vo} = 0.23$) segment of the O-cell test pile, whereas an alpha value of 0.8 was calculated for the more over-consolidated clay ($S_u/\sigma'_{vo} = 0.4$) segment of the head down bored pile loading test. These back-calculated alpha values were approximately double those recommended by FHWA (1999) for bored piles. The FHWA (1999) procedure correlates alpha values to undrained shear strength, S_u , and does not properly account for over-consolidation and embedment depth. On the other hand, back-calculated alpha values closely matched those recommended by API (2000). This agreement is attributed to the API (2000) method correlating alpha to S_u/σ'_{vo} , instead of just S_u . This allows it to consider the effect of over-consolidation and embedment depth.

The back-calculated beta coefficients for the O-cell test pile were 0.25, 0.40, and 0.25 for the upper silty sand with permanent steel casing, the underlying sand, and underlying clay, respectively (Figure 13). The back-calculated beta coefficients within the over-consolidated clay of the head-down bored pile loading test was about 0.32.

The LCPC method fit, “ca-LCPC” in Figure 13, was achieved by using q_t cone stress instead of q_c and disregarding all imposed limits on the shaft resistance, plus applying a multiplier of 1.6 in the normally consolidated clay. No adjustment (multiplier of 1) was required for the LCPC method in the sandy layers. A multiplier of 1.35 was required to fit the shaft resistance in the over-consolidated clay in the head-down bored pile loading test. The fit of the E-F method, “ca-EF” in Figure 13, was achieved by a multiplier of 1.4 above 44 m depth and more than 2 below.

4.0 SUMMARY AND CONCLUSIONS

Pile loading tests at two bridge sites in British Columbia have been described. At both sites, relatively long piles were founded in near normally consolidated sediments. At the W.R. Bennett Bridge site, the sub-soils were lacustrine fine silty sands and silts, whereas at the Golden Ears Bridge site the bearing soils were dominantly marine clayey silts and silty clays. At both locations, pile capacities, calculated prior to the loading tests using various published procedures, varied by more than a factor of two. Design procedures that provided a good fit to loading test results at one of the bridge sites did not work well at the other. These case histories clearly demonstrated the importance of conducting pile loading tests and/or pile driving analyses (PDA) when installing piles in unfamiliar soils. The tests also provided much insight on pile-soil behaviour.

Additional conclusions from the loading tests at the W.R. Bennett Bridge site were:

- Open and closed-toe piles (similar to the tested piles) have similar dynamic capacity
- Vibratory driving of the upper half of the pile did not affect capacity
- PDA/CAPWAP and the static loading test gave similar total capacities
- Residual loads (loads locked into the pile when there is no applied load at the pile head) from pile installation are significant (64% of toe capacity and approaching available shaft resistance in this case) and knowledge of them is required to get the correct load distribution on the pile from the loading test. Residual loads do not affect the total pile capacity. However, as they affect the resistance distribution, proper assessment of residual load is important when extrapolating data from a pile test to piles of other length or diameter.

- The installation method can have a significant effect on residual loads in the pile. Residual loads due to static jacking were almost double those due to impact driving. This effect was also captured numerically. It is believed that dynamic oscillations from driving reduce the residual values from their maximum. The reduction in residual load due to re-striking the piles after the static test seemed to corroborate this.
- Cyclic loading between half and three quarters of the failure load did not cause significant load oscillation at the test pile toe. It is postulated that this may be the case for piles with similar axial stiffness to the test pile, as long as the pile shaft capacity is greater than the oscillation amplitude.
- Developed residual load and general pile behaviour observed in the pile loading test program could be simulated with a relatively simple elastic plastic dynamic numerical model.

Additional conclusions from the static tests at the Golden Ears Bridge site were:

- Pile capacities calculated using the API (2000) alpha method matched those back-calculated from both the head-down and O-cell loading tests. The API approach correlates alpha to the ratio of the undrained shear strength to initial effective stress (S_u/σ'_{vo}) instead of just undrained shear strength (S_u) and thus compensates for embedment and over-consolidation effects. Both the CPT (LCPC) and the CPTU (E-F) cone sounding methods underestimated the pile shaft resistance in the clay soils, and alpha values recommended by FHWA (1999) underestimated by approximately 50% the shaft capacity of piles in clay at this site.
- The back-calculated beta-coefficients ranged from 0.25 through 0.32 for the bored piles within the normally consolidated and over-consolidated clay, respectively, at this site. Within the normally consolidated soils, the beta-coefficient was approximately equal to (S_u/σ'_{vo}).

It should be noted that the correlations and back-calculated shaft resistance parameters presented in this paper are for the specific construction methodologies and site conditions, and they may not apply to other sites and construction projects.

ACKNOWLEDGEMENTS

For the W.R. Bennett Bridge test program, Westmar Consultants Inc. (Worley Parsons) was the prime consultant, Macleod Geotechnical Ltd. (now EXP Services Inc.) the geotechnical consultant, and Griffiths Pile Driving the contractor to the Ministry of Transportation for the pile load test. The authors thank Malcolm MacFaden and Peter Peart for their valiant and successful repair of the two strain gages at the bottom of the 55m deep pipe pile, Dean Polvi of RST Instruments Ltd. for instrumentation, Turgot Ersoy and Don Gillespie of MoT for input to the loading

test design and PDA testing, and Victor Szabo for supervising the pile loading tests and compiling data.

For the Golden Ears Bridge project, the authors wish to acknowledge Golden Crossing Constructors Joint Venture (Bilfinger Berger Canada and CH2M Hill Canada) and BC Translink (The Owner). The work by Loadtest Inc. for conducting the O-cell loading test is acknowledged. Special thanks go to Mr. Stefan Proeck and Michael Buehler from Bilfinger Berger, to Trevor Lumb from Trow Associates Inc., and to Makram Sabbagh from AMEC Inc.

REFERENCES

- Amini, A., Fellenius, B.H., Sabbagh, M., Naesgaard, and, Buehler, M., 2008. "Pile Loading Test at Golden Ears Bridge," 61st Canadian Geotechnical Conference, Canadian Geotechnical Society, Edmonton, Alberta.
- API, RP 2A-WSD, 1993. "Recommended Practice for Planning, Designing and Constructing Fixed Offshore Platforms - Working Stress Design, 20th edition." American Petroleum Institute.
- API 2000. "Recommended Practice for Planning, Designing, and Constructing Fixed Offshore Platforms - Working Stress Design, 21st Edition." American Petroleum Institute 01-Dec-2000 242 p.
- Bustamante, M., Gianeselli, L., 1982. "Pile bearing capacity predictions by means of static penetrometer (CPT)." Proc., 2nd European Symposium on Penetration Testing, ESOPT-II, Amsterdam, The Netherlands, Vol. 2, 493-500.
- CFEM, 2006. Canadian Foundation Engineering Manual, 4th Edition, Canadian Geotechnical Society, c/o BiTech Publishers, Richmond, B.C.
- De Ruiter, J., and Beringen, F.L., 1979. "Pile foundations for large North Sea Structures." *Mar. Geotech.*, 3(3), 267-314.
- Eslami, A. and Fellenius, B.H., 1997. "Pile capacity by direct CPT and CPTu methods applied to 102 case histories." *Can. Geotech. J.*, 34(6) 886-904.
- Eyles N., Mullins, H., and Hine, A.C., 1990. Thick and fast: Sedimentation in a Pleistocene fjord lake of British Columbia, *Geology*, Vol. 18, pp. 1153-1157.
- FHWA 1999. "Drilled Shafts: Construction Procedures and Design Methods." U.S. Department of Transportation Publication FHWA-IF-99-025. Authors O'Neill, M.W. and Reese, L.C.
- Fulton, R.J., 1975. "Quaternary geology and geomorphology, Nicola-Vernon area, British Columbia." Geological Survey of Canada, Memoir 380.
- Fellenius, B.H., 2002a. "Determining the resistance distribution in piles Part 1". Notes on shift of no-load reading and residual load, *Geotechnical News*, 20(2) pp. 23-27.
- Fellenius, B.H., 2002b. "Determining the resistance distribution in piles Part 2. Method for determining the residual load." *Geotechnical News* 20(3) pp. 25-29.
- Fellenius, B.H., 2009. "Basics of foundation design, a text book". Revised Electronic Edition, [www.Fellenius.net], 330 p.
- Fellenius, B.H., Bozozuk, M., and Samson, L., 1978. Soil disturbance from pile driving in sensitive clay. *Canadian Geotechnical Journal* 15(3) 346-361

- Fellenius, B.H., Harris, D., and Anderson, D.G., 2004. Static loading test on a 45 m long pipe pile in Sandpoint, Idaho. *Canadian Geotech. J.* 41(4) 613-628.
- Hunter A.H. and Davisson M.T., 1968. Measurements of pile load transfer. *Proceedings of Symposium on Performance of Deep Foundations*, San Francisco, June 23-28, 1968, American Society for Testing and Materials, ASTM, Special Technical Publication, STP 444, pp. 106-117.
- ITASCA, 2005. "FLAC - Fast langrangian analysis of continua, Version 5.0." ITASCA Consulting Group Inc., Minneapolis, Minnesota.
- Mouta da Costa, L., Danziger, B.R., and Lopes, F.R., 2001. "Prediction of residual driving stresses in piles." *Can. Geotech. J.* 38(1) 410-421.
- Meyerhoff, G.G., 1976. "Bearing capacity and settlement of pile foundations. The Eleventh Terzaghi Lecture." November 5, 1975. ASCE, *Journal of Geotechnical Engineering*, Vol. 102, GT3, pp. 195-228.
- Naesgaard, E., Uthayakumar, M., Ersoy, T. and Gillespie, D., 2006. "Pile load test for W.R. Bennett Bridge." 59th Canadian Geotechnical Conference, Canadian Geotechnical Society, Vancouver, B.C., October.
- Nasmith, H., 1962. "Late glacial history and surficial deposits of the Okanagan Valley, British Columbia." BC Department of Mines and Petroleum Resources, Bulletin No. 46.
- Nordlund, R.L., 1963. "Bearing capacity of piles in cohesionless soils", *ASCE J. of Soil Mech. and Found. Engng.* 89(SM3) 1-35.
- Osterberg, J.O., 1989. "A new device for load testing driven piles and drilled shafts separates friction and end bearing". *Proceedings of Deep Foundations Institute, International Conference on Piling and Deep Foundations*, London, May 15-18, pp. 421-427.
- Osterberg, J.O., 1998. "The Osterberg load test method for drilled shaft and driven piles. The first ten years." *Great Lakes Area Geotechnical Conference. Seventh International Conference and Exhibition on Piling and Deep Foundations*, Deep Foundation Institute, Vienna, June 15-17, 17 p.
- Schmertmann, J.H., 1978. "Guidelines for cone penetration test, performance, and design." Rep. No. FHWA-TS-78-209, U.S. Department of Transportation, Washington, D.C., 145 p.